The Astronomical Journal, 126:2048–2059, 2003 October

CONTRIBUTIONS TO THE NEARBY STARS (NSTARS) PROJECT: SPECTROSCOPY OF STARS EARLIER THAN M0 WITHIN 40 PARSECS: THE NORTHERN SAMPLE. I.

R. O. Gray
Department of Physics and Astronomy, Appalachian State University, Boone, NC 28608;
grayro@appstate.edu

C. J. Corbally
Vatican Observatory Research Group, Steward Observatory, 933 North Cherry Avenue, Tucson, AZ 85721-0065;
corbally@as.arizona.edu

R. F. Garrison
David Dunlap Observatory, P.O. Box 360, Station A, Richmond Hill, ON L4C 4Y6, Canada;
garrison@astro.utoronto.ca

and

M. T. McFadden and P. E. Robinson
Department of Physics and Astronomy, Appalachian State University, Boone, NC 28608;
mcfaddnm@pm.appstate.edu
Received 2003 May 8; accepted 2003 July 11

ABSTRACT

We have embarked on a project, under the aegis of the Nearby Stars (NStars)/*Space Interferometry Mission* Preparatory Science Program, to obtain spectra, spectral types, and, where feasible, basic physical parameters for the 3600 dwarf and giant stars earlier than M0 within 40 pc of the Sun. In this paper, we report on the results of this project for the first 664 stars in the northern hemisphere. These results include precise, homogeneous spectral types, basic physical parameters (including the effective temperature, surface gravity, and overall metallicity [M/H]), and measures of the chromospheric activity of our program stars. Observed and derived data presented in this paper are also available on the project's Web site.

Key words: stars: abundances — stars: activity — stars: fundamental parameters — stars: statistics — surveys

On-line material: machine-readable table

1. INTRODUCTION

The three institutions represented by the authorship of this paper are cooperating on a project under the NASA/JPL Nearby Stars/*Space Interferometry Mission* Preparatory Science Program to obtain spectroscopic observations of all 3600 main-sequence and giant stars with spectral types earlier than M0 within a radius of 40 pc. We are obtaining blue-violet spectra at classification resolution (1.5–3.6 Å) for all of these stars. These spectra are being used to obtain homogeneous, precise, MK spectral types. In addition, these spectra are being used in conjunction with synthetic spectra and existing intermediate-band Strömgren *uvby* and broadband *VRI* photometry to derive the basic astrophysical parameters (the effective temperature, gravity, and overall metal abundance [M/H]) for many of these stars. We are also using these spectra, which include the Ca II K and H lines, to obtain measures of the chromospheric activity of the program stars on the Mount Wilson system. The purpose of this project is to provide data that will permit an efficient choice of targets for both the *Space Interferometry Mission* (*SIM*) and the projected *Terrestrial Planet Finder* (*TPF*). In addition, combination of these new data with kinematic data should enable the identification and characterization of stellar subpopulations within the solar neighborhood.

Observations for this project are being carried out on the 1.9 m telescope of the David Dunlap Observatory in a northern polar cap (decl. $> +50^\circ$), the 0.8 m telescope of the Dark Sky Observatory ($-10^\circ \leq$ decl. $\leq +50^\circ$), the 2.3 m Bok Telescope of Steward Observatory ($-30^\circ \leq$ decl. $\leq -10^\circ$), and the 1.5 m telescope at Cerro Tololo Inter-American Observatory (decl. $\leq -30^\circ$), although there is considerable overlap between all of these samples. In this paper, we report on results for the first 664 stars, all observed at the Dark Sky Observatory.

2. OBSERVATIONS AND CALIBRATION

The observations reported in this paper were all made on the 0.8 m telescope of the Dark Sky Observatory (Appalachian State University), situated on the escarpment of the Blue Ridge Mountains in northwestern North Carolina. The Gray/Miller classification spectrograph was employed with two gratings, with 600 and 1200 grooves mm^{-1}, and a thinned, back-illuminated 1024×1024 Tektronix CCD operating in the multipinned-phase mode. The observations were made with a 100 μm slit, which corresponds to approximately 2″ at the focus of the telescope; average seeing at the Dark Sky Observatory (DSO) is about 3″. The 100 μm slit with the two gratings yields 2 pixel resolutions of 3.6 and 1.8 Å and spectral ranges of 3800–5600 and 3800–4600 Å, respectively. The lower resolution spectra were used primarily for the late-type stars in the sample (later than G5), whereas the higher resolution spectra were used primarily for the earlier-type stars. An FeAr hollow-cathode comparison lamp was used for the wavelength

calibration, and all of the spectra were reduced with standard methods using IRAF.[1]

The 1.8 Å resolution spectra were rectified using an X Window System program, xmk19, written by one of us (R. O. G.) and were used in that format for both spectral classification and for the determination of the basic physical parameters. For the late-type stars rectification is problematic, as no useful "continuum" points can be identified. In addition, the energy distribution contains useful information for both the spectral classification and the determination of the basic physical parameters. We have therefore made an attempt to approximately flux-calibrate the 3.6 Å resolution spectra even though they were obtained with a narrow slit. During the course of our observations for this project at DSO over the past 3 years, we have, at intervals of a few months, made observations of spectrophotometric standards at a variety of air masses. These standard observations have been used to approximately remove the effects of atmospheric extinction and to calibrate the spectrograph throughput as a function of wavelength. Except for observations made at high air masses (>1.8 air masses), this procedure yields calibrations of *relative* fluxes with accuracies on the order of ±10%. While this is sufficient for the purposes of accurate spectral classification, the determination of the basic physical parameters requires a more accurate flux calibration. This we have achieved by "photometrically correcting" the fluxes using Strömgren photometry. The DSO 3.6 Å resolution spectra have a spectral range that includes three of the four Strömgren bands, *v*, *b*, and *y*. We perform numerical photometry on these spectra and use the absolute flux calibration of the Strömgren system (Gray 1998) to derive flux corrections at the effective wavelengths of the three photometric bands. Interpolation and extrapolation of these corrections yield flux corrections over the entire observed spectrum. From comparison with spectrophotometric observations in the literature, we find that this procedure yields not only relative but also absolute fluxes with accuracies of about ±3% over nearly the entire spectral range. Fortunately, most of our program stars with spectral types of K3 and earlier have Strömgren photometry. For the later-type stars without Strömgren photometry, other considerations (see § 4) preclude the derivation of basic physical parameters from our spectra, and so the lack of accurate fluxes is not otherwise limiting.

All of the spectra obtained for this project are available on the project's Web site.[2] Rectified spectra from DSO have an extension of .r18 or .r36 depending on the resolution. The 3.6 Å resolution flux spectra, which have not been photometrically corrected, are normalized at a common point (4503 Å) and have an extension of .nor, whereas photometrically corrected spectra are available in a normalized format (.nfx) and in terms of absolute fluxes (.flx) in units of ergs s^{-1} cm^{-2} $Å^{-1}$. Spectra obtained at the other observatories (see § 1) are also available on this Web site and will be the subject of future papers.

[1] IRAF is distributed by the National Optical Astronomy Observatory, which is operated by the Association of Universities for Research in Astronomy, Inc. under cooperative agreement with the National Science Foundation.

[2] See http://stellar.phys.appstate.edu/.

3. SPECTRAL CLASSIFICATION

The spectral types for the stars in this paper were obtained using MK standard stars selected from the list of "Anchor Points of the MK System" (Garrison 1994), the Perkins catalog (Keenan & McNeil 1989), and, for late K- and early M-type dwarfs, Henry et al. (2002). A list of the standards used (and the actual spectra) can be found on the project Web site.

The program stars were first classified independently on the computer screen by eye (using the graphics program xmk19) by at least two of the authors, and then the spectral types were compared and iterated until complete agreement was obtained. There are significant overlaps between the samples observed with the four telescopes employed for this project, to ensure homogeneity of our spectral types over the entire sky. This homogeneity is further ensured by a significant overlap in the MK standards used for each sample, and close scrutiny of the nonoverlapping standards to verify consistency. The spectral types for the first sample of 664 stars from the northern hemisphere observed at DSO are recorded in Table 1. These spectral types are multidimensional, as they include not only the temperature and luminosity types, but also indices indicating abundance peculiarities and the degree of chromospheric activity.

Chromospheric activity is evident in our spectra through emission reversals in the cores of the Ca II K and H lines and, in more extreme situations, infilling and emission in the hydrogen lines. We have indicated these different levels of chromospheric activity in the spectral types with the following notation: "(k)" indicates that slight emission reversals or infilling of the Ca II K and H lines is visible; "k" indicates that emission reversals are clearly evident in the Ca II K and H lines but these emission lines do not extend above the surrounding (pseudo-) continuum; "ke" indicates emission in the Ca II K and H lines above the surrounding (pseudo-) continuum, usually accompanied with infilling of the Hβ line; and "kee" indicates strong emission in Ca II K and H, Hβ, and perhaps even Hγ and Hδ. Because chromospherically active stars tend also to be variable, the chromospheric activity "type" will also vary. We have therefore noted the observation date in the notes to Table 1 for those stars that have been designated either "ke" or "kee." Stars of special astrophysical interest have been noted in § 6, as well as in the notes to Table 1. Specific dates of observation for all of the stars observed on this project can be found in the "footers" of the spectra themselves, available on the project Web site.

Spectral types are important to this project because (1) they provide the first detailed look at our data and enable us to pick out peculiar and astrophysically interesting stars, and (2) accurate spectral types yield beginning values for our determination of the basic physical parameters and provide a check on the derived physical parameters. In addition, our spectral types enable us to refine the census of stars within 40 pc of the Sun. Figure 1 shows an H-R diagram based on the spectral types in Table 1 and *Hipparcos* parallaxes (ESA 1997). Note the sharp lower edge to the main sequence and the good separation between the luminosity classes. Note, however, the handful of stars scattering below the main sequence. These stars, without exception, have large parallax errors. Most of these stars are in double and multiple systems, explaining the parallax errors. Our

TABLE 1
SPECTRAL TYPES, BASIC PHYSICAL PARAMETERS, AND CHROMOSPHERIC INDICES

HIP	BD/HD	SpT	N1	$T_{\rm eff}$	log g	ξ_t	[M/H]	N2	$S_{\rm MW}$	log $R'_{\rm HK}$	AC	N3
171.....	224930	G5 V Fe−1	...	5502	4.27	(1.0)	−0.64	...	0.183	−4.880	I	1.8
400.....	225261	G9 V	...	5250	4.40	(1.0)	−0.43	...	0.148	−5.094	I	3.6
518.....	123	G4 V	*	5718	4.50	(1.0)	0.06	...	0.257	−4.644	A	1.8
544.....	166	G8 V	...	5412	4.41	(1.0)	0.07	...	0.379	−4.458	A	3.6
677.....	358	B8 IV–V Hg Mn	...	13098	3.91	(2.0)	(0.0)	*	...	...	...	...

NOTES.—Table 1 is presented in its entirety in the electronic edition of the Astronomical Journal. A portion is shown here for guidance regarding its form and content. See also § 6 for notes on astrophysically interesting stars. The column headings have the following meanings: HIP stands for the designation in the *Hipparcos* Catalogue (ESA 1997); HD/BD for the HD or the BD designation; SpT for the spectral type—note that some long spectral types are continued in the notes. An asterisk in column "N1" refers to a note on the spectral type. Headings $T_{\rm eff}$, log g, ξ_t, and [M/H] refer to the basic physical parameters—the effective temperature (kelvins), the logarithm of the surface gravity, the microturbulent velocity in kilometers per second, and the overall metal abundance on a logarithmic scale, where [M/H] = 0.00 refers to solar metallicity (note that if any of these quantities is enclosed in parentheses, it was held fixed in the SIMPLEX solution). An asterisk in column "N2" refers to a note on the SIMPLEX solution; a "K" in this column indicates that the method used to determine the basic physical parameters was that adopted for the G and K giants. $S_{\rm MW}$ is the chromospheric activity index on the Mount Wilson system; log $R'_{\rm HK}$, a measure of the chromospheric flux in the Ca II K and H lines; "AC" indicates the chromospheric activity class—(VI) very inactive; (I) inactive; (A) active; (VA) very active. Column "N3" indicates the resolution of the spectrum in angstroms used for the measurement of $S_{\rm MW}$ and log $R'_{\rm HK}$. An asterisk in this column indicates a note on chromospheric activity.

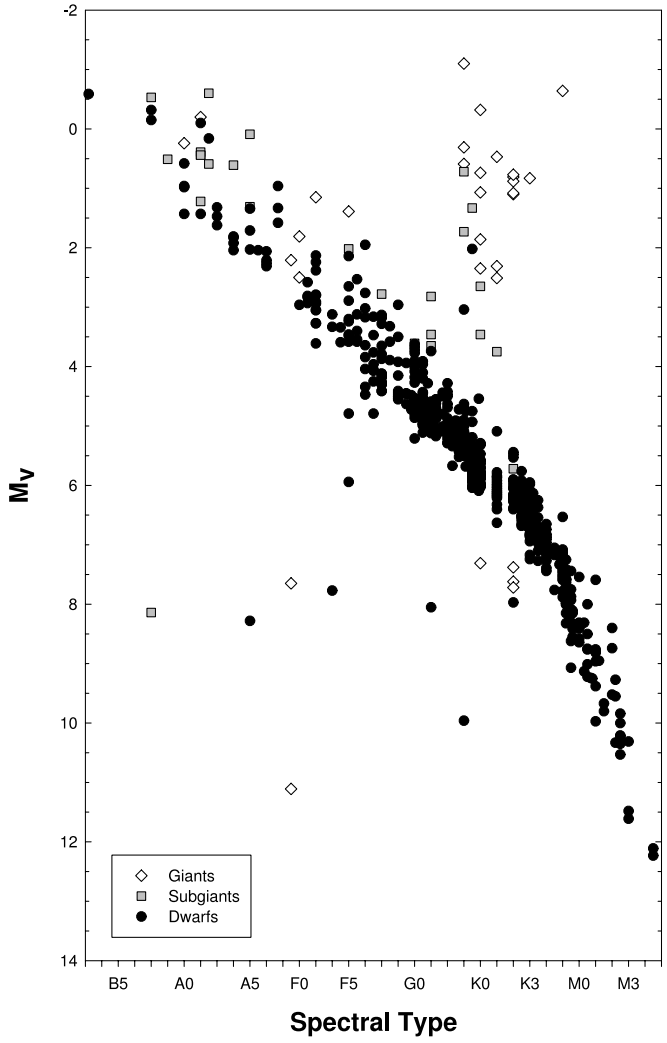

FIG. 1.—Observational H-R diagram formed from the spectral types of the 664 stars reported in this paper. The absolute magnitudes, M_V, are calculated using *Hipparcos* (ESA 1997) parallaxes. The stars scattering below the main sequence in this figure all have large parallax errors and are listed in Table 2. These stars are all evidently more distant than 40 pc.

spectral types confirm that these stars lie significantly beyond 40 pc. These stars are listed in Table 2.

4. BASIC PHYSICAL PARAMETERS

An important goal of this project is to derive the basic physical parameters—the effective temperature, the surface gravity, and the overall metallicity—for as many of our program stars as possible.

4.1. *Determination of the Basic Physical Parameters*

To determine these parameters, we use a technique similar to that devised by Gray, Graham, & Hoyt (2001), which fits the observed spectra and fluxes from medium-band (Strömgren *uvby*) and broadband (Johnson and Johnson-Cousins *VRI*) photometry and, when available, *IUE* spectra, to synthetic spectra and fluxes. The fit is achieved by minimizing a χ^2 statistic formed from the point-to-point squared differences between the synthetic and observed spectra plus a similar sum over the squared differences between the observed and synthetic fluxes. The sum of the squared differences for the spectra are given approximately 3 times the weight of the sum of the squared differences over the fluxes in

TABLE 2
STARS BEYOND 40 PARSECS IDENTIFIED BY MK CLASSIFICATION

HIP	BD/HD	Spectral Type	$\pi \pm \sigma_\pi$[a] (mas)	$d_{\rm MK}$[b] (pc)
1663	1651	kA7hA9mF0 III	46.72 ± 20.16	290
1692	1690	K2 III	43.42 ± 33.05	340
7765	10182	K2 III	61.30 ± 36.67	320
24502	33959C	F5 V	39.77 ± 22.40	95
30362	256294	B8 IVp	48.08 ± 13.63	1050
30756	257498	K0 IIIb	55.52 ± 33.89	230
35389	+18°1563	A5 V	52.47 ± 28.98	370
76051	+10°2868C	G2 V CH−0.3	44.59 ± 20.41	90
84581	−07°4419B	A9 III	100.89 ± 43.18	275
116869	+13°5158B	G8 V^+	44.81 ± 60.22	80
117042	222788	F3 V	53.88 ± 32.40	170

[a] *Hipparcos* parallaxes and errors (ESA 1997).
[b] Approximate distance based on the MK type.

the final χ^2. The synthetic spectra and fluxes are based on Kurucz (1993) ATLAS9 stellar atmosphere models (calculated *without* convective overshoot), and the synthetic spectra are computed with the spectral synthesis program SPECTRUM (Gray & Corbally 1994).[3] Since the publication of the Gray et al. (2001) paper, much effort has been put into improving the spectral line list used by SPECTRUM, including updating the oscillator strengths with the latest critically evaluated values from the NIST Web site.[4] Full details can be found on the SPECTRUM Web site.

The minimization of the χ^2 statistic is carried out by the multidimensional downhill simplex algorithm "amoeba" (Press et al. 1992). We have modified the Gray et al. (2001) technique by introducing a graphical front end ("xfit16") to this algorithm, which allows the user to visually find an approximate global solution, which is then polished using the SIMPLEX engine. Any of the four basic physical parameters ($T_{\rm eff}$, log g, the microturbulent velocity ξ_t, and the overall metal abundance [M/H]) may be held fixed or allowed to vary in the solution. A further improvement on the Gray et al. technique is the possibility to introduce observed fluxes not only from Strömgren *uvby* photometry, but also from Johnson and Johnson-Cousins *VRI* photometry and from *IUE* spectra. In addition, xfit16 can rotationally broaden the synthetic spectra and thus is capable of treating even stars with high v sin i. The graphical program xfit16 can access multiple libraries of synthetic spectra for each of the different data sets in the project (for instance, the two dispersions from DSO, spectra from CTIO, the David Dunlap Observatory, and the Bok Telescope of Steward Observatory). The program xfit16 allows the user not only to verify that the solution obtained is the global solution, but also to visually judge the quality of the solution and to decide whether any of the input data are defective. While xfit16 allows the user to deredden the observed fluxes, the reddening for all of our program stars was assumed to be zero.

For the B- and early A-type stars in our program, we utilized observed fluxes from the Strömgren u, b, and y bands and, when available, *IUE* spectra obtained from the MAST *IUE* Web site.[5] The flux calibration used for the Strömgren photometry is that of Gray (1998). Because the metallic lines in these stars are quite weak and thus do not have much leverage on the solution, the solution was first optimized with [M/H] held fixed at 0.00, and then [M/H] was adjusted manually until good agreement was obtained visually with the metallic line strengths. The solution was then reoptimized and [M/H] readjusted if necessary. For these stars, a microturbulent velocity of 2 km s^{-1} was assumed. The *IUE* spectra, when available, were valuable in determining [M/H] because line blanketing is much greater in the ultraviolet. An example of a SIMPLEX/xfit16 solution for an early A-type star, HD 47105, is shown in Figure 2.

For the late A-, F-, and early G-type stars, *IUE* spectra were generally not available, and so the flux solution was constrained by fluxes from Strömgren u, b, and y

[3] See http://www.phys.appstate.edu/spectrum/spectrum.html.
[4] See http://physics.nist.gov.
[5] See http://archive.stsci.edu/iue/.

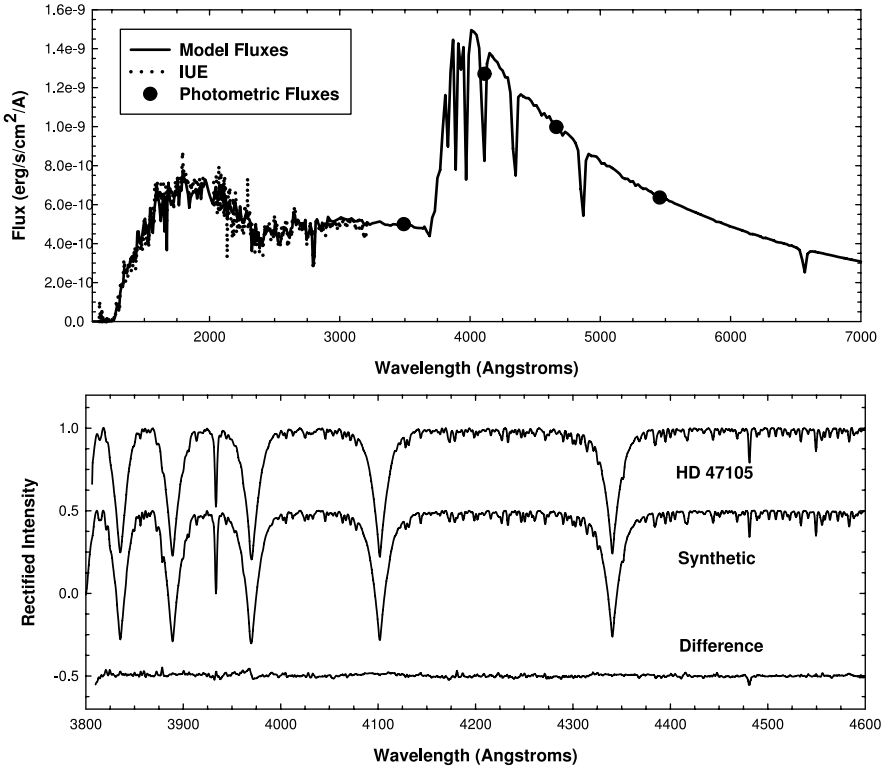

FIG. 2.—SIMPLEX solution for the early A-type star HD 47105. The top panel shows the fit with respect to photometric fluxes (Strömgren *uvby*) and ultraviolet fluxes from *IUE* spectra. The bottom panel shows the fit with the observed spectrum; the difference between the observed and synthetic spectrum is seen at the bottom of the panel.

photometry. For these stars, all four physical parameters were allowed to vary to derive the final solution.

For the late G- and K-type dwarfs, a number of points had to be taken into consideration to achieve good solutions. First, for these cooler stars the flux solution is not well constrained by observed fluxes from the Strömgren bands, but it is necessary to include photometric fluxes from the red and the near-infrared in the form of Johnson and/or Johnson-Cousins *VRI* photometry. We have used the absolute flux calibration for the Cousins *R* and *I* bands of Bessell (1990). To ensure uniformity, when only Johnson *VRI* photometry was available for a star, we used the equations of Fernie (1983) to transform Johnson $V-R$ and $V-I$ colors to Johnson-Cousins $V-R$ and $V-I$ colors and then used Bessell's calibration. Unfortunately, many of our late G- and K-type stars do not have either Johnson or Johnson-Cousins *VRI* photometry. We have found, however, that for *dwarf* stars the following equations are able to predict Johnson-Cousins $V-R$ and $V-I$ colors from Strömgren $b-y$ colors in the range $0.4 < b-y < 0.8$ with an accuracy of 0.015 mag for $V-R$ and 0.03 mag for $V-I$:

$$V-R = 1.30(b-y) - 0.17 ,$$
$$V-I = 2.32(b-y) - 0.25 .$$

We can detect only a slight dependence on metallicity in these relationships, well within the errors for stars with $[M/H] > -0.7$. By happy circumstance, most of the very metal-weak stars in our sample have *VRI* photometry. The Kurucz fluxes in the Strömgren *u* band do not reproduce well the observed fluxes in the late G- and K-type stars, and so the *u*-band fluxes are not used in the SIMPLEX solution for these stars.

It is unfortunate that neither the energy distributions of the late G- and K-type dwarfs nor our classification spectra strongly constrain the surface gravity for these stars. In the B-, A-, F-, and even early G-type stars, the Balmer jump strongly constrains the surface gravity, but this feature is too weak to serve this purpose in the late G- and K-type stars. The normal MK luminosity criteria in the K-type stars (the strength of the CN band, and certain lines of ionized species such as Sr II λ4077 and Y II λ4376—both used in ratio with adjacent Fe I lines) do not offer sufficient leverage in the SIMPLEX solutions to yield accurate ($\pm$0.10 dex) values for $\log g$ in the *dwarfs*. We have found that allowing $\log g$ to be a free parameter in the SIMPLEX solution for the late G- and K-type dwarfs often results in an unreliable value (usually too low) for that parameter in the final solution. We have therefore constrained $\log g$ to the value implied by the *Hipparcos* parallax and the mass-luminosity relationship (Gorda & Svechnikov 1998). We have further constrained $\xi_t = 1.0$ km s^{-1}. With these constraints, we generally obtain good-to-excellent solutions for dwarfs of spectral type K3 and earlier. An example of such a fit for a K3 dwarf can be seen in Figure 3.

Later than K3, however, the quality of the synthetic spectra and fluxes, especially in the spectral region used (3800–5600 Å), begins to deteriorate for the dwarf stars. It is clear that in this spectral region, for $T_{\rm eff} < 4500$ K, a significant contributor to the continuous opacity is missing in both ATLAS9 and SPECTRUM. Synthetic fluxes normalized and matched in the red to observed fluxes similarly normalized are too high compared with the observed fluxes in the blue-violet, and synthetic line strengths in the blue-violet are too strong. This persists even when both synthetic and observed spectra are normalized at a common point in the blue-violet. This effect is seen even in the NextGen models

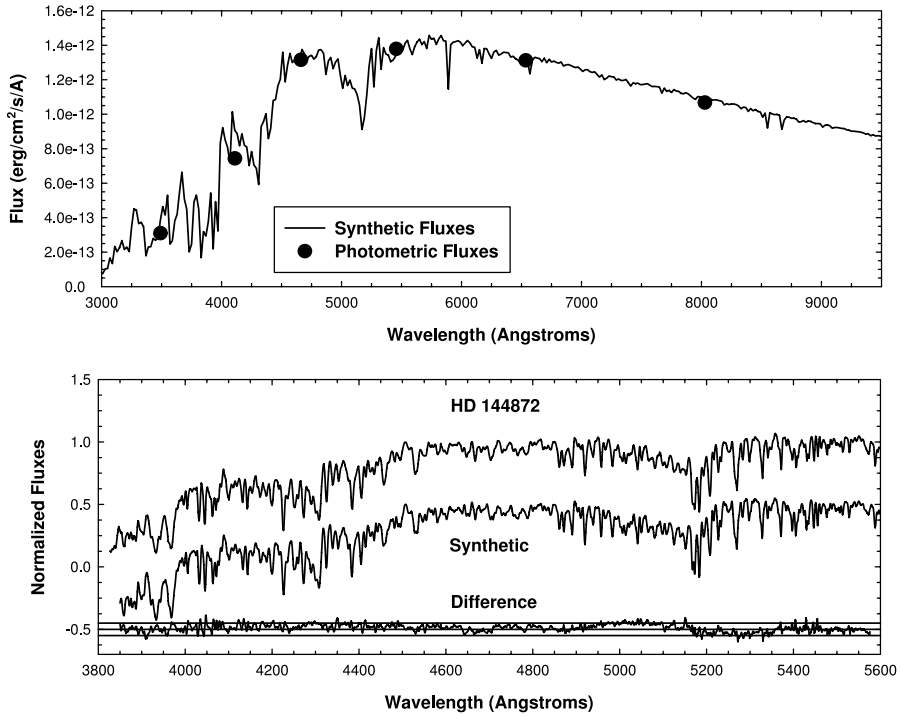

FIG. 3.—Example of a SIMPLEX fit for a K3 dwarf, HD 144872. The difference spectrum (synthetic minus observed) is shown at the bottom of the lower panel; the parallel lines indicate errors of $\pm$5% in the flux. The top panel shows the fit to the observed photometric fluxes; the illustrated points are, from left to right, Strömgren *u*, *v*, *b*, and *y* fluxes and Johnson-Cousins *R* and *I* fluxes. The Strömgren *u* flux is not used in the solution.

and synthetic spectra of Hauschildt, Allard, & Baron (1999). This missing opacity in the blue-violet region is reminiscent of a similar effect found in K giant stars in the violet by Short & Lester (1994). Short & Lester suggested that this missing violet continuous opacity might be supplied by photodissociation of MgH. However, Weck et al. (2003) have recently calculated this continuous opacity; it is about an order of magnitude too small to explain the observed effect. Other possible culprits include CaH and the O^- ion, as CaH has a dissociation energy similar to that of MgH and the ionization energy of O^- is about 2 eV. This discrepancy between observed and synthetic spectra and fluxes unfortunately prevents us from calculating basic physical parameters for dwarf stars later than K3 from our spectra.

For the late G- and K-type giants and subgiants, it is likewise necessary to introduce certain constraints to derive good solutions. For most of the G and K giants and subgiants in our program $V-K$ photometry exists, and so we have elected to use the infrared flux method (IRFM) of Blackwell & Lynas-Gray (1994) to derive starting conditions and constraints for the SIMPLEX solutions. For the few giants without $V-K$ photometry, we have found that the following equations can be used to predict $V-K$ colors to sufficient accuracy (± 0.06 mag) for our purposes:

$$V-K = 3.80(b-y) - 0.02 ,$$

$$V-K = 1.39(B-V)^2 - 0.98(B-V) + 1.87 ,$$

valid for $0.55 < b-y < 0.90$ and $0.90 < B-V < 1.50$, respectively. The IRFM uses the following polynomial to predict the effective temperature (for $V-K > 0.35$):

$$T_{\rm eff} = 8862 - 2583(V-K) + 353.1(V-K)^2 . \qquad (1)$$

The luminosity of the star may be determined using the *Hipparcos* parallaxes with bolometric corrections (Flower 1996), and the radius may be determined from the Stefan-Boltzmann law. We then determine the mass for the star using the evolutionary tracks of Claret & Giménez (1995) for $Z = 0.01$ (because many of the giants are slightly metal-weak) and thence the surface gravity. The normal procedure with the giants is then to constrain the $T_{\rm eff}$ to the IRFM value in the SIMPLEX solution, constrain $\xi_t = 1.0$ km s^{-1}, begin with log g as calculated above, and manually adjust [M/H] so that the line strengths in the synthetic spectrum are approximately correct. The simplex algorithm is then allowed to polish the solution. The basic physical parameters for this first set of program stars may be found in Table 1.

4.2. *Reliability of the Basic Physical Parameters*

A thorough discussion of the errors associated with the SIMPLEX method may be found in Gray et al. (2001), but since a number of improvements to both the spectral synthesis program SPECTRUM and to the SIMPLEX method have been made since the publication of that paper, a review of the errors is warranted.

An excellent internal check on the precision of the SIMPLEX effective temperatures is afforded by a comparison with our spectral types. Figure 4 shows a plot of $T_{\rm eff}$ versus the spectral type running number (Keenan 1984) for the dwarfs in our sample. A polynomial fit yields a scatter of ± 115 K, part of which is attributable to errors in the spectral types and the width of the spectral boxes. This

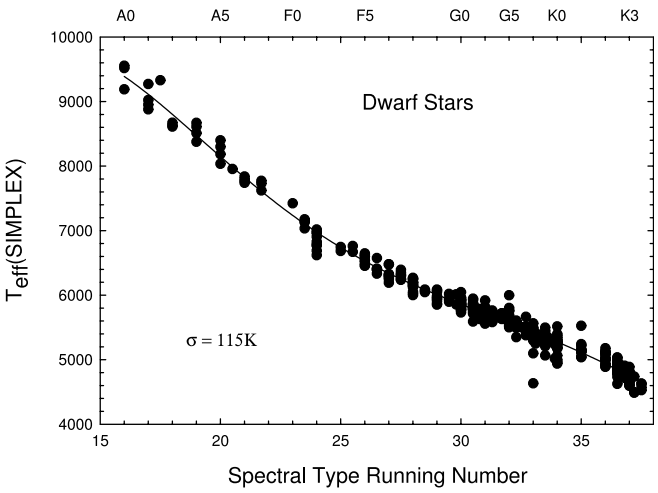

FIG. 4.—Correlation between the SIMPLEX effective temperatures and the spectral type for the dwarf stars in the present sample. The scatter in this relationship is ± 115 K and sets an upper limit on the random error in the SIMPLEX effective temperatures.

polynomial yields the effective temperature–spectral type calibration for dwarf stars in Table 3. We conservatively estimate a random error in the SIMPLEX effective temperatures of ± 80 K. For an external check, we may compare the SIMPLEX effective temperatures with those derived from the IRFM (Blackwell & Lynas-Gray 1994). To do this, we have selected those dwarfs in Table 1 that have $V-K > 0.35$ and have plotted (Fig. 5) $V-K$ against the SIMPLEX effective temperatures. The solid line in that figure shows the IRFM calibration (see eq. [1]). As can be seen, the agreement is excellent; the scatter around the IRFM calibration is ± 115 K, and a close comparison suggests that the SIMPLEX temperatures are systematically only 30 K hotter than the IRFM temperatures.

It is of interest to compare the SIMPLEX effective temperatures with those in the Cayrel de Strobel, Soubiran, & Ralite (2001) catalog (hereafter the [Fe/H] catalog), which contains determinations of $T_{\rm eff}$, log g, and [Fe/H] from the literature based on high-resolution spectroscopy. This catalog contains only data derived from digital detectors (i.e., older photographic determinations have been removed from this version of the catalog), but the data are not otherwise critically assessed. The [Fe/H] values in this catalog are derived using a number of techniques, ranging from the curve-of-growth method to spectral synthesis.

TABLE 3

AN EFFECTIVE TEMPERATURE CALIBRATION FOR DWARF STARS

Spectral Type	$T_{\rm eff}$ (K)	Spectral Type	$T_{\rm eff}$ (K)	Spectral Type	$T_{\rm eff}$ (K)
A2.....	8800	F3.....	6740	G5.....	5580
A3.....	8480	F5.....	6530	G8.....	5430
A5.....	8150	F7.....	6250	G9.....	5350
A7.....	7830	F8.....	6170	K0.....	5280
A9.....	7380	F9.....	6010	K1.....	5110
F0.....	7240	G0.....	5860	K2.....	4940
F1.....	7100	G1.....	5790	K3.....	4750
F2.....	6980	G2.....	5720		

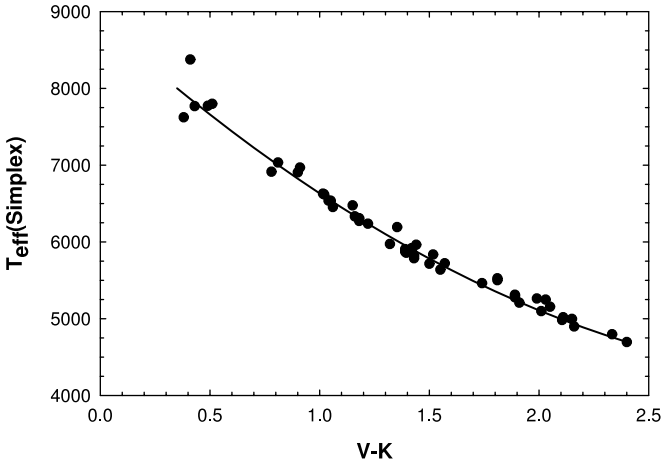

FIG. 5.—Comparison of SIMPLEX effective temperatures with the IRFM calibration. This comparison constitutes an external check on the SIMPLEX effective temperatures. The solid line is the IRFM polynomial (eq. [1]). The scatter of SIMPLEX temperatures around this curve is 115 K, and the systematic difference over this range of effective temperatures does not appear to exceed 30 K. The IRFM temperatures are essentially independent of theoretical models.

Figure 6 shows that for the G- and K-type stars in common, there is good agreement between the SIMPLEX values of $T_{\rm eff}$ and those of the [Fe/H] catalog ($\sigma = 100$ K, with a negligible zero-point difference), but in the F-type stars there is a systematic difference in the sense that the SIMPLEX effective temperatures are about 100 K hotter than the literature values. There is, however, good agreement at G0 and for the early F-type stars.

This systematic difference in the F-type stars can be traced to a faulty convective-overshoot algorithm included in the ATLAS9 stellar atmosphere program (Kurucz 1993). This

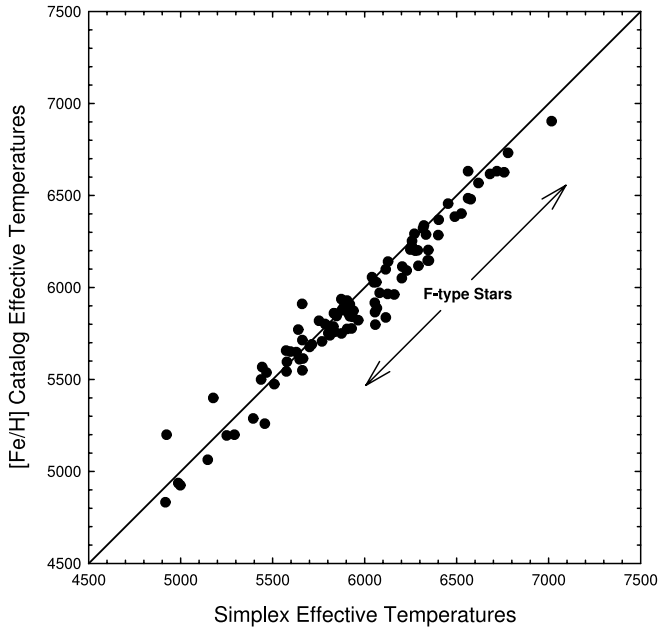

FIG. 6.—Comparison of the SIMPLEX effective temperatures with those in the Cayrel de Strobel et al. (2001) [Fe/H] catalog. The systematic difference in the F-type stars is probably due to a defective convective-overshoot algorithm used in the published ATLAS9 models (Kurucz 1993). This has been corrected in the models used in the SIMPLEX solutions.

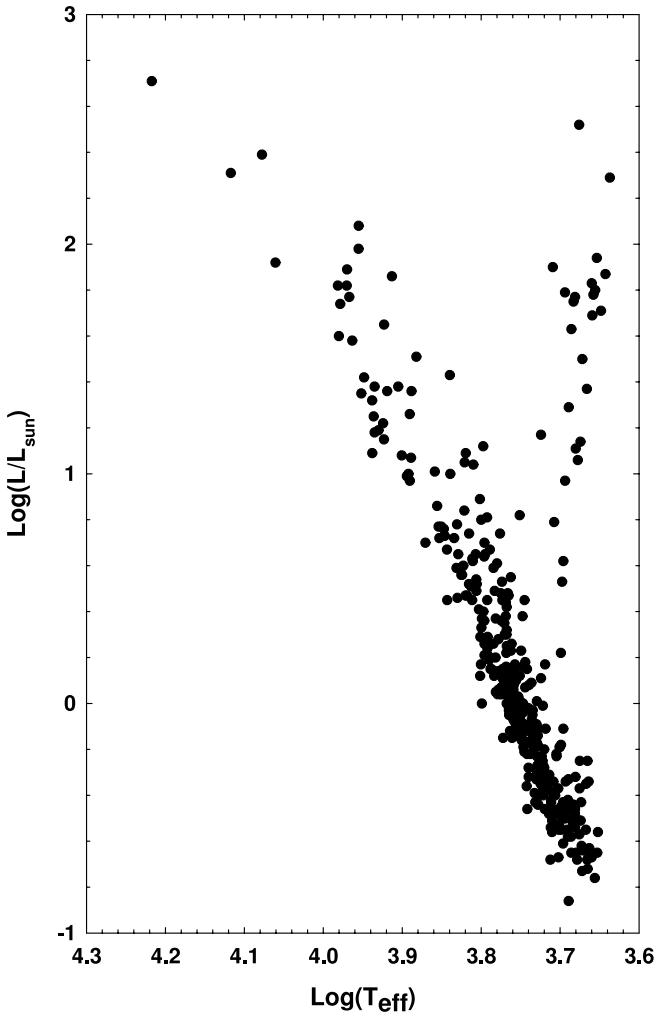

FIG. 7.—Astrophysical H-R diagram based on SIMPLEX physical parameters.

faulty algorithm introduces a systematic error in the structure of the stellar atmosphere models of the partially convective F-type star atmospheres (Smalley & Kupka 1997). This produces a distortion in the temperature scale of the F-type stars, which is unfortunately reflected in many of the determinations listed in the [Fe/H] catalog.

We have recomputed the ATLAS9 models for the F-type stars with convective overshoot turned off using the implementation of ATLAS9 by M. Lemke[6] and used these models in the spectral libraries employed by SIMPLEX (see Gray et al. 2001 for further details). Figure 7 shows an astrophysical H-R diagram based on the SIMPLEX physical parameters.

An important parameter for those who would use our data for the nearby stars in exoplanet searches is the metallicity [M/H] of the star. There is some indication that planets are found preferentially around stars with higher-than-solar metallicities (Gonzalez 1999).

Comparing the SIMPLEX [M/H] values with mean [Fe/H] values from the [Fe/H] catalog for the stars in common, we find small but significant zero-point differences (see

[6] Available at http://www.sternwarte.uni-erlangen.de/ftp/michael/atlas-lemke.tgz.

TABLE 4
ZERO-POINT DIFFERENCES: $[Fe/H]_{CATALOG}$ MINUS $[M/H]_{SIMPLEX}$

Stellar Type	Resolution (Å)	Zero Point
F and G dwarfs	1.8	0.02
G and K dwarfs.....	3.6	0.05
G and K giants.....	3.6	0.23

Table 4). The zero-point differences for the dwarfs are generally small, but the zero-point difference for the G and K giants is quite large and requires some discussion. Many of the determinations in the [Fe/H] catalog for G and K giants were made with stellar atmosphere models calculated with the MARCS code or its predecessors (Gustafsson et al. 1975), and this may indicate a systematic difference between the Kurucz models and the MARCS models. However, we expect that this systematic difference in the giants has more to do with the fact that the abundance determinations in the [Fe/H] catalog were largely carried out at wavelengths longer than 5000 Å, and for the most part in the red, whereas the SIMPLEX solutions use blue-violet spectra (3800–5600 Å). We have noted above discrepancies in line strengths in the dwarfs between observed and synthetic spectra in the blue-violet for $T_{\rm eff} < 4500$ K, and we expect that we are seeing a similar phenomenon in the giants, although to a lesser degree (note that many of our giants have $T_{\rm eff} < 4500$ K). Missing continuous opacity in the blue-violet would lead to greater line strengths in the models and, thus, systematically negative values for [M/H].

Having applied the zero-point corrections in Table 4 to the SIMPLEX [M/H] values, we find excellent agreement with the [Fe/H] catalog values (see Fig. 8). The [M/H] values in Table 1 have had these corrections applied. The random error in the comparison is only ±0.09 dex, hardly larger than the internal scatter in the [Fe/H] catalog (≈0.08 dex, illustrated with error bars on one point in the figure). This is an impressive result, considering that the [Fe/H] catalog values were determined from high-resolution spectra. Such accurate and homogeneous [M/H] values for a large sample of nearby stars will make possible a number of investigations, including examination of the hypothesis that planets are found preferentially around metal-rich stars. We will consider this hypothesis in Paper II of this series.

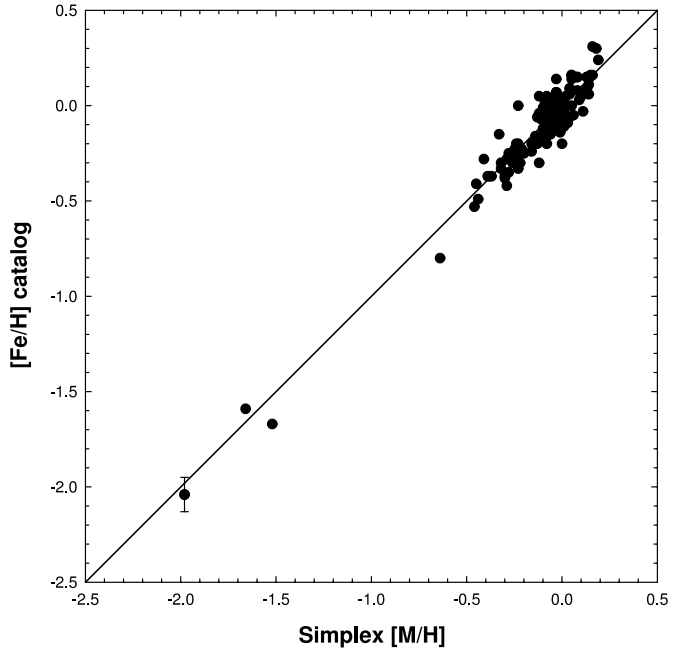

FIG. 8.—Comparison between the SIMPLEX [M/H] (overall metal abundance) and mean [Fe/H] values from the Cayrel de Strobel et al. (2001) [Fe/H] catalog. The scatter in the comparison is 0.09 dex, similar to the scatter for single stars in the [Fe/H] catalog, ≈0.08 dex.

5. CHROMOSPHERIC EMISSION

All of the spectra obtained for this project include the Ca II K and H lines and thus can be used to obtain measures of the chromospheric emission, as emission from the chromosphere can be detected in the cores of these very strong lines. This is an important measurement, as chromospheric emission can be an indication of the age of a star and its binary status. An age determination can be important for exoplanet searches, as an indication of a young age for a star might preclude observations using interferometric or coronagraphic techniques as a consequence of the complicating effects of zodiacal light from a remnant protoplanetary disk.

We measure the chromospheric emission in our program stars by calculating relative fluxes in four wavelength bands (see Fig. 9), two of which are centered on the Ca II K and H lines. The other two bands measure fluxes in the "continuum" just shortward and longward of Ca II K and H. These bands are essentially identical to those used in the Mount Wilson chromospheric activity survey program (Baliunas et al. 1995), except that the bands centered on Ca II K and H are wider (4 Å) than those used at Mount Wilson (1 Å) because our spectra are of lower resolution. Our instrumental chromospheric emission index is calculated, like the Mount Wilson index, with the following equation:

$$S = 5\frac{\mathrm{K} + \mathrm{H}}{\mathrm{C}_1 + \mathrm{C}_2} \ .$$

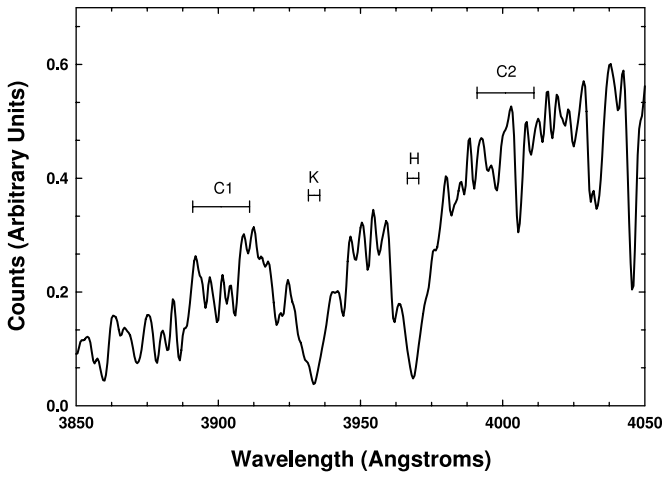

FIG. 9.—Numerical passbands utilized in the calculation of the chromospheric activity index S. Two bands, each 4 Å wide, are centered on the Ca II K and H lines. The C_1 and C_2 bands measure the flux in the continuum in 20 Å wide segments of the spectrum on either side of the K and H lines.

TABLE 5
CHROMOSPHERIC ACTIVITY CALIBRATION STARS

HD	$\langle S_{MW} \rangle$	HD	$\langle S_{MW} \rangle$	HD	$\langle S_{MW} \rangle$
9562	0.136	100563	0.202	159332	0.144
16160	0.226	106516	0.208	178428	0.154
16673	0.215	114378	0.244	182101	0.216
18256	0.185	114710	0.201	187013	0.154
22049	0.496	115383	0.313	188512	0.136
26923	0.287	120136	0.191	190360	0.146
29645	0.140	126053	0.165	194012	0.198
33608	0.214	131156A	0.461	201091	0.658
43587	0.156	136202	0.140	201092	0.986
45067	0.141	141004	0.155	206860	0.330
78366	0.248	142373	0.147	212754	0.140
81809	0.172	143761	0.150	216385	0.142
82885	0.284	152391	0.393	217014	0.149
89744	0.137	154417	0.269		
100180	0.165	158614	0.158		

This index is defined in such a way that it is insensitive to the local slope of the continuum in the vicinity of the Ca II K and H lines. Thus, we find that this index is identical (within a few thousandths) whether we use flux-calibrated spectra or uncalibrated raw counts. We determine this index by using a feature in the spectral classification program xmk19 that allows the user to shift the spectrum in wavelength to exactly align the K and H bands with the cores of the Ca II K and H lines and which then carries out a numerical integration over the four bands. To ensure accuracy in the numerical integration over these bands, we resample the spectrum into 0.1 Å bins.

To place this chromospheric index on the Mount Wilson scale, it is necessary to use "standard" stars to derive a transformation equation. Unfortunately, all solar-type stars show some variability in the chromospheric index, and those with higher values of S are generally more variable. What this means is that unless one has observations taken near in time to Mount Wilson observations, it is impossible to derive an exact transformation equation. One, however, can derive a transformation of sufficient accuracy to characterize stars as active, inactive, etc., by selecting from the Mount Wilson list (Baliunas et al. 1995) those stars that do not show long-term secular trends or irregular behavior as calibration stars. The stars we have selected for this purpose are listed in Table 5. The resulting calibration for the 1.8 Å resolution spectra is shown in Figure 10. To fit the trend in Figure 10, we have employed a cubic fit given by

$$S_{MW} = -39.976 S_{18}^3 + 43.335 S_{18}^2 - 11.592 S_{18} + 1.041$$

for $S_{18} < 0.361$. For $S_{18} \geq 0.361$ (the inflection point of the above cubic), the curve is extended with a straight line, having the slope of the cubic at the inflection point:

$$S_{MW} = 4.067 S_{18} - 0.845 .$$

This straight line is also used to extrapolate to values of S_{MW} outside the range represented by the calibration stars.

We estimate the errors in this transformation allow a determination of the Mount Wilson activity index, S_{MW}, to an accuracy of 5% with larger uncertainties (including unknown systematic errors) for $S_{MW} > 0.8$. To ensure compatibility of the derived S_{MW} values from the 3.6 Å resolution spectra with the 1.8 Å spectra, we first transform the instrumental S_{36} values onto the instrumental S_{18} system and then use the above calibration. The transformation from the S_{36} system to the S_{18} system is determined by using stars observed with both resolutions within a time frame of a few months. This transformation is linear, with a slope of unity and a zero-point difference of 0.039. The scatter in this transformation, an indication of the precision with which we can measure S_{MW}, is ± 0.010.

The S_{MW} index measures the flux in the core of the Ca II K and H lines, but there are both photospheric and chromospheric contributions to this flux. The photospheric flux may be removed approximately following the procedure of Noyes et al. (1984), who derive a quantity $R_{HK} \propto F_{HK}/\sigma T_{eff}^4$, where F_{HK} is the flux per square centimeter in the H and K bandpasses. The quantity R_{HK} can be derived from S_{MW} by modeling the variation in the continuum fluxes (in bands C_1 and C_2) as a function of effective temperature (using $B-V$ as a proxy). R_{HK} must then be further corrected by subtracting off the photospheric contribution in the cores of the H and K lines. The logarithm of the final quantity

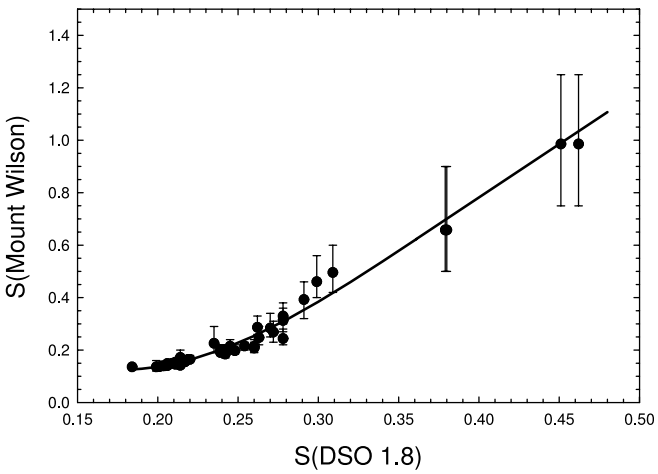

FIG. 10.—Calibration between the instrumental S_{18} chromospheric activity index and the Mount Wilson S-index. The "error bars" represent the range of variation shown by the stars in Baliunas et al. (1995). The solid line shows the adopted calibration.

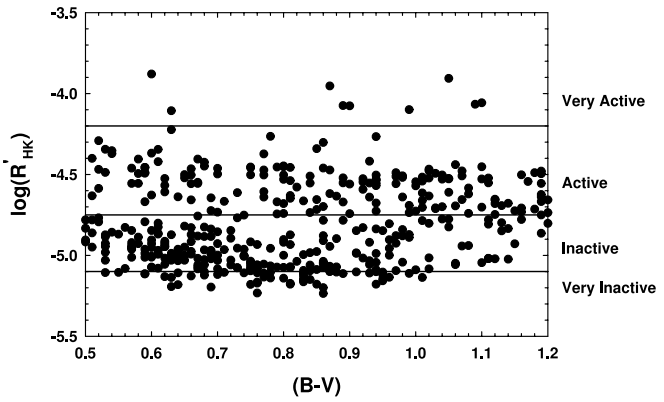

FIG. 11.—Plot of the chromospheric flux parameter log R'_{HK} vs. the $B-V$ color. This diagram allows the classification of stars into the chromospheric activity categories "very inactive," "inactive," "active," and "very active." All but one of the "very active" stars are well-known flare stars or BY Draconis or RS CVn variables. The exception is HIP 90035 (see text and Fig. 13).

R'_{HK} is then a useful measure of the chromospheric emission, essentially independent of the effective temperature. We have calculated R'_{HK} for all of our dwarf program stars later than F5 and earlier than M0 with $B-V$ photometry. While the conversion of S_{MW} into R'_{HK} becomes increasingly uncertain for $B-V > 1.20$ (approximately spectral type K5), we have carried this calculation out for stars as late as K8. Both the S_{MW} and the log R'_{HK} indices are tabulated for our program stars in Table 1.

We follow Henry et al. (1996) in employing log R'_{HK} to classify stars into "very inactive," "inactive," "active," and "very active" categories (see Fig. 11 and Table 1). The distribution of stars in Figure 11 is similar to that in Figure 7 of Henry et al. (1996), except that their study had a bias toward G dwarfs and did not go to as late a spectral type as our project.

Figure 12 shows a histogram of the log R'_{HK} values for the program stars with $0.5 < B-V < 0.9$. This distribution may be compared directly with Figure 8 of Henry et al. (1996). It is clear that the distribution is bimodal, with a peak near log $R'_{HK} = -5.0$ and another peak near -4.5, very similar to that found by Henry et al. We have used the Levenberg-Marquardt method (Press et al. 1992) to fit a double-Gaussian model to this distribution; the result is shown in Figure 12 with the residuals from the fit illustrated in the bottom panel. It is clear that this double-Gaussian model (peaks at log $R'_{HK} = -4.996$ and log $R'_{HK} = -4.536$, with FWHM of 0.266 and 0.352, respectively—again very similar to the results of Henry et al.) fits the distribution within the errors, with the possible exception of one bin, at log $R'_{HK} = -5.1$. This bin shows an excess (a 2.5 σ result) of stars. An examination of Table 1 shows that out of the 36 stars in this bin, only two are metal-weak ([M/H] < -0.50) and three are slightly evolved (either classified as subgiants or having log $g \leq 4.00$). The remaining stars in this bin are apparently normal, near–solar metallicity, chromospherically inactive dwarfs. This result suggests that the excess stars in this bin and in all of the bins representing very inactive stars (log $R'_{HK} < -5.1$) may be due to dwarfs in a Maunder minimum phase (see also Henry et al. 1996, and Table 6 for a list of possible solar-metallicity Maunder minimum dwarfs). However, as these excesses are only marginally significant statistically with the current sample, we will defer discussion of this point to later papers in this series.

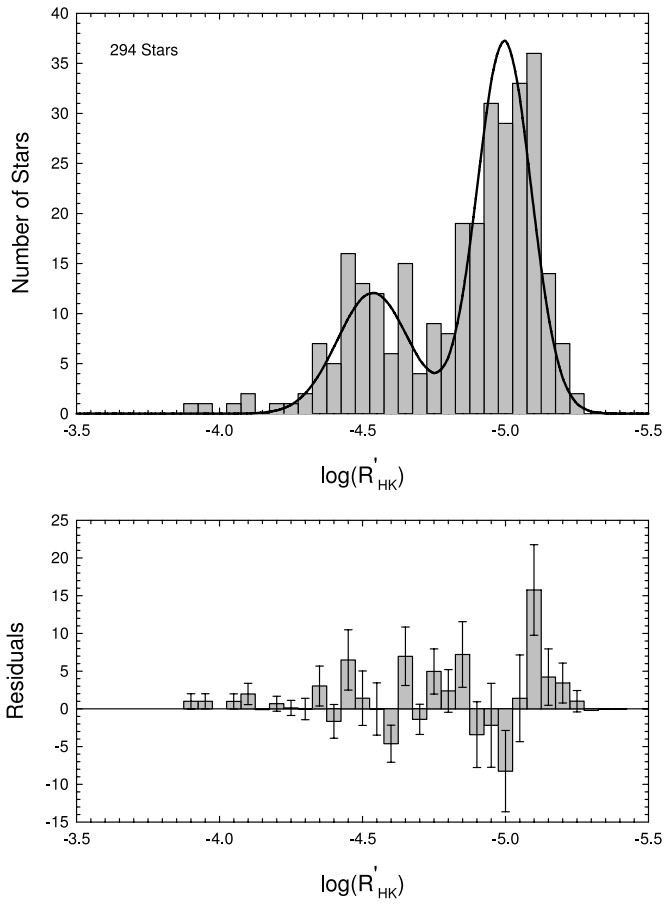

FIG. 12.—Distribution of the chromospheric flux parameter log R'_{HK} for stars with $0.50 < B-V < 0.90$. The distribution is clearly bimodal, with the main peak representing chromospherically inactive stars, and the secondary peak chromospherically active stars. The double-Gaussian curve is a fit to the distribution. The bottom panel shows the residuals associated with this fit. With the exception of the bin centered at log $R'_{HK} = -5.1$, the fit is within the errors. The excess number of stars at log $R'_{HK} = -5.1$ is discussed in § 5.

Most of the stars in the "very active" category in Figure 11 are well-known variables of either the BY Draconis or RS CVn types. These stars are named in the notes to Table 1. Two exceptions are HIP 90035 (=BD +01°3657), which shows strong emission in Ca II K and H but which is not a

TABLE 6

POSSIBLE SOLAR-METALLICITY MAUNDER MINIMUM DWARFS

HIP	BD/HD	Spectral Type	[M/H]	log R'_{HK}
9269	12051	G9 V	0.00	−5.134
35872	57901	K3$^-$ V	0.00	−5.135
39064	65430	K0 V	−0.20	−5.110
42499	73667	K2 V	−0.15	−5.127
67246	120066	G0 V	0.14	−5.193
70873	127334	G5 V CH+0.3	−0.03	−5.118
88348	164922	G9 V	0.00	−5.141
101345	195564	G2 V	−0.09	−5.196
116085	221354	K0 V	0.00	−5.149

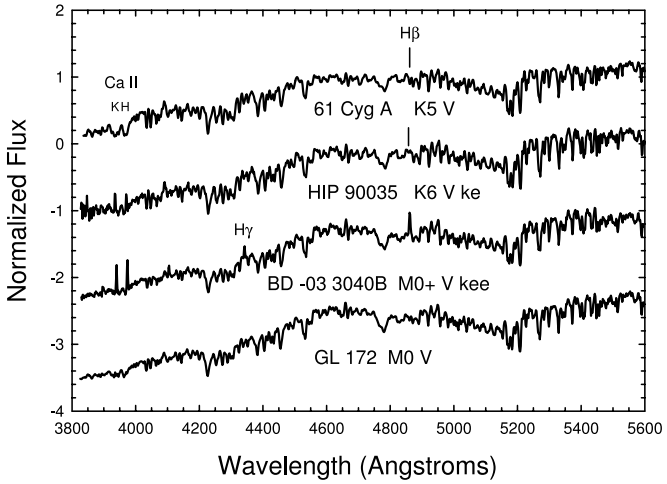

FIG. 13.—Some astrophysically interesting stars. HIP 90035 = BD +01°3657 is a chromospherically very active star that has not been classified as a flare, BY Draconis, or RS CVn star. Note the strong emission (in comparison with the K5 V standard 61 Cyg A) in Ca II K and H, and the infilling of the Hβ line with emission. Likewise, BD −03°3040B is a chromospherically active early M dwarf, not yet classified in the literature as an emission-line star, showing strong emission in Ca II K and H as well as Hβ, Hγ, and Hδ.

known variable, and BD −03°3040B, which shows strong emission in Ca II and the hydrogen lines (see the notes in § 6 and Fig. 13).

6. NOTES ON ASTROPHYSICALLY INTERESTING STARS

HIP 7585 = HD 9986: Solar twin. Note how closely the SIMPLEX basic physical parameters resemble those of the Sun. This star is also chromospherically inactive and has a classification spectrum indistinguishable from that of the Sun. However, in a speckle survey of G dwarfs (Horch et al. 2002), this star, while not resolved, was listed as a suspected nonsingle star.

HIP 16209 = LHS 173: This star is clearly metal-weak, but abundance-independent criteria place the spectral type of this star near to K7. At that spectral type, the MgH band at 4780 Å appears of nearly normal strength. This luminosity (gravity) sensitive feature therefore suggests an unusually high gravity. Classified as a subdwarf K7 star by Gizis (1997).

HIP 53910 = HD 95418: Some sharp lines, Fe II λ4233 enhanced. May be a mild shell star.

BD −03°3040B: Strong emission in Ca II K and H and the hydrogen lines. This star is not a known variable, but it has been detected in X-rays by *ROSAT* (Mason et al. 1995). Observed on 2001 January 31. Double with HD 96064. HD 96064 is chromospherically active as well, suggesting that this is a young binary system. (See Fig. 13.)

HIP 90035 = BD +01°3657: Very active chromospherically, but not a known variable. Observed on 2000 August 8. Detected in the extreme-ultraviolet (Lampton et al. 1997). A probable new BY Draconis variable. (See Fig. 13.)

7. CONCLUSIONS

We have presented a database for 664 dwarf and giant stars earlier than M0 within 40 pc of the Sun that includes new, homogeneous spectral types, basic physical parameters, and measures of chromospheric activity. Similar data on the remaining 2935 solar-type nearby stars will be presented in subsequent papers in this series. The goals of this project are to characterize the stellar population in the solar neighborhood and to provide data that will be useful in the selection of targets for the *Space Interferometry Mission* and the *Terrestrial Planet Finder* mission. As an example of how this database could be helpful in selection of targets for discovering terrestrial planets around solar-type stars, Table 7 contains stars from the database that satisfy the following criteria:

1. Solar-type dwarfs with spectral types from F8 to G8;
2. Solar metallicity: $[M/H] > -0.10$ (following the hypothesis of Gonzalez [1999] that planets are found preferentially around metal-rich stars—the validity of this hypothesis will be tested in Paper II);
3. Chromospherically inactive or very inactive: chromospheric activity can be an indicator of a young age, so to find terrestrial planets with extraterrestrial life, older stars should be selected, and in addition, a young age for the star might preclude observation by a spacecraft such as *TPF* because of the presence of excessive zodiacal light in the system;
4. Single and nonvariable.

It should be noted that 13 of the stars in Table 1 already have known planets. These are HD 19994, 46375, 75732, 89744, 137759, 143761, 145675, 186427, 190360, 210277,

TABLE 7
CANDIDATE STARS FOR TERRESTRIAL PLANET SURVEYS

HIP	BD/HD	Spectral Type
1499	1461	G3 V
7585	9986	G2 V
7918	10307	G1 V
14150	18803	G6 V
14632	19373	F9.5 V
14954	19994	F8.5 V
24813	34411	G1 V
30545	45067	F8 V
41484	71148	G1 V
49081	86728	G4 V
49756	88072	G3 V
56242	100180	F9.5 V
61053	108954	F9 V
67246	120066	G0 V
70873	127334	G5 V CH+0.3
73100	132254	F8$^-$ V
74605	136064	F8 V
79862	147044	G0 V
85042	157347	G3 V
85810	159222	G1 V
89474	168009	G1 V
90864	171067	G6 V
94981	181655	G5 V
96895	186408	G1.5 V
100017	193664	G0 V
101345	195564	G2 V
102040	197076	G1 V
103682	199960	G1 V

217014, 217107, and 222404. These stars have not been included in Table 7.

The data presented in this paper are currently available on the project's Web site, and work is continuing on the remaining stars in the project, which will be the subject of future papers in this series. As more results become available and the statistical significance of our results improves, we intend to examine detailed features of the distribution of chromospheric activity among solar-type stars and the validity of the hypothesis that exoplanets are found preferentially around metal-rich stars, and to point out stars of astrophysical interest and of interest to the *SIM* and *TPF* missions.

This work has been carried out under contract with NASA/JPL (JPL contract 526270) and has been partially supported by grants from the Vatican Observatory and Appalachian State University. This research made use of the SIMBAD database, operated at CDS, Strasbourg, France. We would also like to thank Jean-Claude Mermilliod for his assistance in the compilation of photometry for our database. Many thanks to graduate student Kelly Kluttz and to undergraduate students Chris Jackolski, John Robertson, Corey Yost, and Kate Hix, all at Appalachian State University, for assistance in observing.

REFERENCES

Baliunas, S. L., et al. 1995, ApJ, 438, 269
Bessell, M. S. 1990, PASP, 102, 1181
Blackwell, D. E., & Lynas-Gray, A. E. 1994, A&A, 282, 899
Cayrel de Strobel, G., Soubiran, C., & Ralite, N. 2001, A&A, 373, 159
Claret, A., & Giménez, A. 1995, A&AS, 114, 549
Dorren, J. D., & Guinan, E. F. 1994, ApJ, 428, 805
ESA. 1997, The Hipparcos and Tycho Catalogues (ESA SP-1200) (Noordwijk: ESA)
Fernie, J. D. 1983, PASP, 95, 782
Flower, P. J. 1996, ApJ, 469, 355
Garrison, R. F. 1994, in ASP Conf. Ser. 60, The MK Process at 50 Years, ed. C. J. Corbally, R. O. Gray, & R. F. Garrison (San Francisco: ASP), 3
Gizis, J. E. 1997, AJ, 113, 806
Gonzalez, G. 1999, MNRAS, 308, 447
Gorda, S. Yu., & Svechnikov, M. A. 1998, AZh, 75, 896 (English transl. Astron. Rep., 42, 793)
Gray, R. O. 1998, AJ, 116, 482
Gray, R. O., & Corbally, C. J. 1994, AJ, 107, 742
Gray, R. O., Graham, P. W., & Hoyt, S. R. 2001, AJ, 121, 2159
Gray, R. O., & Kaye, A. B. 1999, AJ, 118, 2993
Gustafsson, B., Bell, R. A., Eriksson, K., & Nordlund, Å. 1975, A&A, 42, 407
Hauschildt, P. H., Allard, F., & Baron, E. 1999, ApJ, 512, 377
Henry, T. J., Soderblom, D. R., Donahue, R. A., & Baliunas, S. L. 1996, AJ, 111, 439
Henry, T. J., Walkowicz, L. M., Barto, T. C., & Golimowski, D. A. 2002, AJ, 123, 2002
Horch, E. P., Robinson, S. E., Ninkov, Z., van Altena, W. F., Meyer, R. D., Urban, S. E., & Mason, B. D. 2002, AJ, 124, 2245
Keenan, P. C. 1984, in The MK Process and Stellar Classification, ed. R. F. Garrison (Toronto: David Dunlap Obs.), 29
Keenan, P. C., & NcNeil, R. C. 1989, ApJS, 71, 245
Kurucz, R. L. 1993, CD-ROM 13, ATLAS9 Stellar Atmosphere Programs and 2 km/s Grid (Cambridge: Smithsonian Astrophys. Obs.)
Lampton, M., Lieu, R., Schmidt, J. H. M. M., Bowyer, S., Voges, W., Lewis, J., & Wu, X. 1997, ApJS, 108, 545
Mason, K. O., et al. 1995, MNRAS, 274, 1194
Noyes, R. W., Hartmann, L. W., Baliunas, S. L., Duncan, D. K., & Vaughan, A. H. 1984, ApJ, 279, 763
Press, W. H., Teukolsky, S. A., Vetterling, W. T., & Flannery, B. P. 1992, Numerical Recipes in C (2d ed.; Cambridge: Cambridge Univ. Press)
Short, C. I., & Lester, J. B. 1994, ApJ, 436, L165
Smalley, B., & Kupka, F. 1997, A&A, 328, 349
Weck, P. F., Schweitzer, A., Stancil, P. C., Hauschildt, P. H., & Kirby, K. 2003, ApJ, 584, 459